http://www.jstage.jst.go.jp/browse/biophysics

BIOPHYSICS

REVIEW

Vol. 9, pp. 91–98 (2013)
doi: 10.2142/biophysics.9.91

Experimental thermodynamics of single molecular motor

Shoichi Toyabe[1] and Eiro Muneyuki[2]

[1]*Systems Biophysics, Faculty of Physics, Ludwig-Maximilians-University Munich, Munich 80799, Germany*
[2]*Department of Physics, Faculty of Science and Engineering, Chuo University, Kasuga, Tokyo 112-8551, Japan*

Received April 18, 2013; accepted June 12, 2013

Molecular motor is a nano-sized chemical engine that converts chemical free energy to mechanical motions. Hence, the energetics is as important as kinetics in order to understand its operation principle. We review experiments to evaluate the thermodynamic properties of a rotational F_1-ATPase motor (F_1-motor) at a single-molecule level. We show that the F_1-motor achieves 100% thermodynamic efficiency at the stalled state. Furthermore, the motor reduces the internal irreversible heat inside the motor to almost zero and achieves a highly-efficient free energy transduction close to 100% during rotations far from quasistatic process. We discuss the mechanism of how the F_1-motor achieves such a high efficiency, which highlights the remarkable property of the nano-sized engine F_1-motor.

Key words: F_1-ATPase, Nonequilibrium physics, Single-molecule experiment

Thermodynamics of a single molecule

Thermodynamics conventionally treats macroscopic quantities and the relations between them. Therefore, "thermodynamics of a single molecule" may sound contradicting. Indeed, being bombarded by thermal motions of the solvent molecules, the quantities involved in a single molecule fluctuate and do not retain definite values[1]. However, it is possible to define thermodynamic quantities such as heat, entropy, internal energy, free energy on the basis of the statistical properties of the stochastic trajectories of a single degree of freedom. When properly defined, they become natural extensions of the corresponding quantities in the conventional thermodynamics and satisfy thermodynamic laws. Furthermore, the conventional thermodynamics laws have been generalized into the forms containing fluctuations like the fluctuation theorems and Jarzynski equality[2–5] and provided fruitful information about the system.

Thermodynamics of a small fluctuating system is especially important for the study of molecular motors since they are chemical engines that convert chemical free energy to mechanical motions. This is more true for the rotational molecular motor F_1-motor since its primary role in cells is the reversible free-energy conversion[6–11]. However, despite the intensive studies of the kinetics and reaction scheme of molecular motors, information about the energetics of molecular motors is quite limited due to the lack of the methodology to study the energetics of nano-sized system experimentally. It is beyond this short review to cover the details of thermodynamics in small fluctuating systems (see recent reviews and books for the details[1,4,5,12,13]). Instead, we show how we can reveal the thermodynamics of a single molecular motor by experiments.

F_1-motor

The $\alpha_3\beta_3\gamma$ sub-complex is the minimum rotational unit of the F_1-motor, which consists of a rotator γ-shaft and a stator $\alpha_3\beta_3$-ring[14–16] (Fig. 1a). When isolated, the F_1-motor hydrolyzes ATP and rotates the γ-shaft against the $\alpha_3\beta_3$-ring unidirectionally[17]. The γ-shaft rotates 120° per ATP hydrolysis without slips[18,19]. On the other hand, F_1-motor forms a complex F_oF_1-ATP synthase with another motor F_o-motor in cells (Fig. 1b). The F_o-motor is embedded in a membrane. Driven by a transmembrane electrochemical potential, protons flow through the F_o-motor and rotates its c-ring unidi-

Corresponding author: Shoichi Toyabe, Systems Biophysics, Faculty of Physics, Ludwig-Maximilians-University Munich, Amalienstr. 54, Munich 80799, Germany.
e-mail: s.toyabe@lmu.de

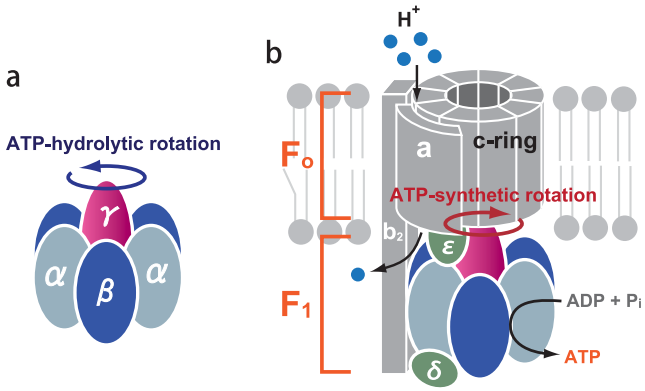

Figure 1 F_1-motor and F_oF_1-ATP synthase. a, The $\alpha_3\beta_3\gamma$ sub-complex of F_1-motor. b, F_oF_1-ATP synthase consists of F_o-motor (ab_2c_n) and F_1-motor ($\alpha_3\beta_3\gamma\delta\varepsilon$). *n* depends on species.

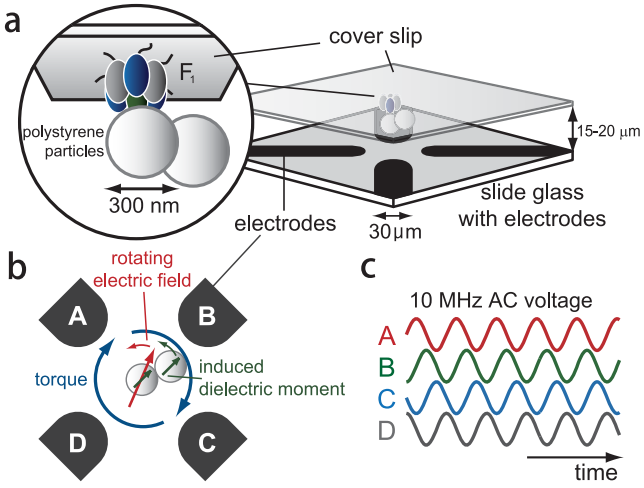

Figure 2 Response measurement of F_1-motor by electrorotation method. a, By adhering the $\alpha_3\beta_3$-ring to a glass surface and attaching a probe of dimeric particles to the γ-shaft, its rotation can be observed under optical microscope. b, Electrorotation method. Four electrodes are patterned on the glass surface. A rotating electric field at a frequency of typically 10 MHz was generated at the center of electrodes by applying sinusoidal voltages with a phase shift of π/2. Dielectric objects in this rotating electric field have a dielectric moment rotating at 10 MHz. The phase delay between the electric field and the dielectric moment results in the torque on the objects. Adapted from ref. 6 with modification.

rectionally. Since the c-ring is connected to the γ-shaft of F_1-motor, the γ-shaft is rotated[20]. The direction of this forced rotation is opposite to that of the ATP-driven rotation. In this case, the F_1-motor synthesizes ATP from ADP and phosphate instead of hydrolyzing ATP.

Response measurement of single molecule

It is essential to measure the thermodynamic quantities like work and heat to reveal the thermodynamic properties of the system. The standard approach to obtain thermodynamic quantities is to measure the response against external load. For example, we control the pressure on a macroscopic piston attached to a cylinder, measure the change of the cylinder volume, and evaluate the work performed on the cylinderfrom the pressure-volume curve. Recent developments in experimental techniques have made it possible to apply essentially the same procedure to the F_1-motor at a single molecule level[6,9,21]. We can probe the rotations of a single F_1-motor molecule under a conventional optical microscope by attaching a submicron-sized object to the rotator γ-shaft and fixing the stator $\alpha_3\beta_3$-ring to a glass surface[17,18] (Fig. 2). Furthermore, we can mechanically control the rotational probe by magnetic tweezers or an electrorotation method.

The magnetic tweezers have been used to trap ferrous particles at a certain angular position by static or electric magnets[11,19,22–24]. The probe feels a harmonic potential around this angular position. We can rotate the probe by rotating the direction of the magnetic field. ATP synthesis under mechanically-forced rotations was demonstrated by using magnetic tweezers[19,23].

On the other hand, the electrorotation method exerts a constant torque on the dielectric probe instead of a trapping torque[6,9,21,25–27]. A constant torque with a torque magnitude independent of the probe motion makes it easier to measure the response function than using the trapping torque by the magnetic tweezers. In this method, alternative-current voltages at a high frequency like 10 MHz are applied on quadrupolar electrodes patterned on a bottom glass surface of the chamber (Fig. 2b). By shifting the phases of these voltages with π/2, an electric field rotating at 10 MHz is generated in the center of the electrodes. Under this rotating electric field, a dipole moment rotating at 10 MHz are induced on the probe particle. Because of the phase delay between the electric field and dipole moment, the probe is subjected to a constant torque. The magnitude of torque is proportional to the square of the voltage amplitude. Therefore, we can control the torque magnitude by changing the voltage. Modulating the voltage temporally, we can induce a time-periodical torque for example. The torque magnitude is also proportional to the volume of the dielectric objects. Note that, by oscillating the direction of the electric field instead of rotating it with a different set of phase shifts of the voltages, we can trap objects at a certain angular position like magnetic tweezers[26].

Rotation under load

Figure 3a shows the rotational trajectory of a single F_1-motor molecule probed by a dimeric plastic particle at low ATP concentration[9]. The F_1-motor rotated in discrete 120° steps. The rate-limiting step, observed as a pause between steps, corresponds to the ATP waiting state; binding of ATP triggers a 120° rotation[18]. When we induced a hindering torque on the probe in the opposite direction of ATP-driven rotation, average duration of the pauses increased, and the

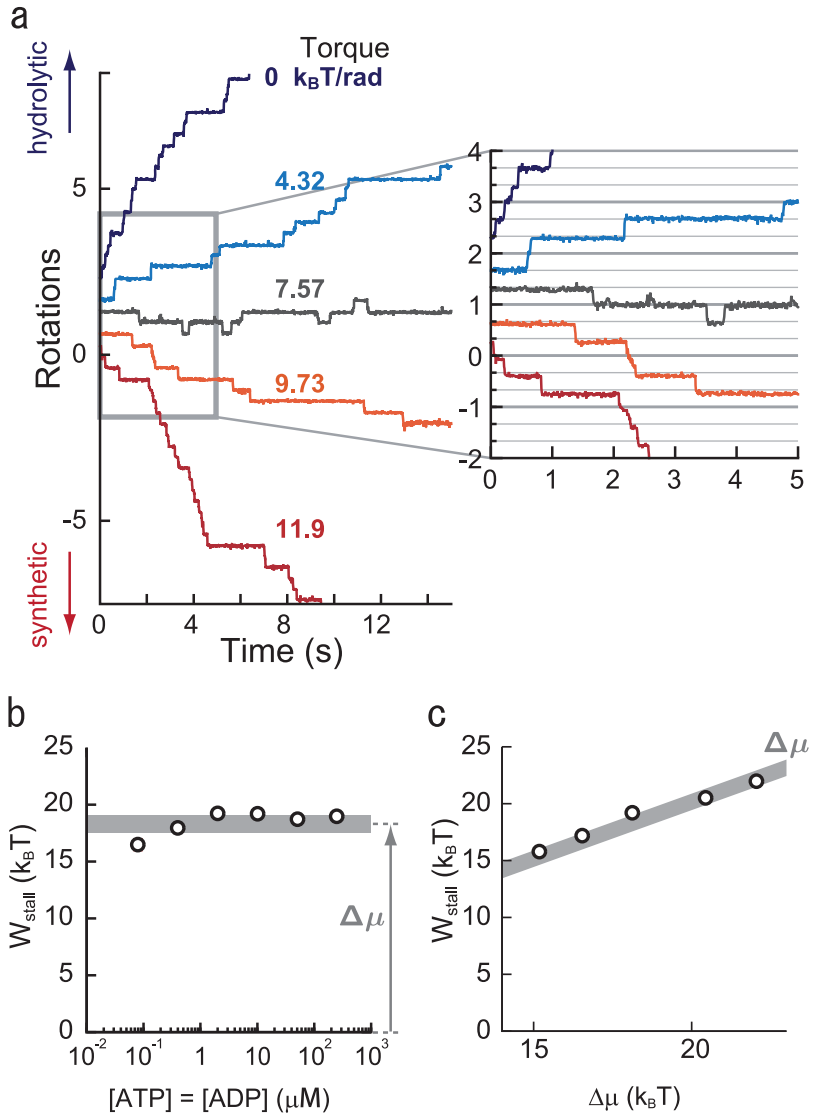

Figure 3 a, Rotational trajectories under external torque (0.4 μM ATP, 4 μM ADP, 1 mM P_i) of the same F_1-motor molecule. b, W_{stall} at [ATP] = [ADP], and [P_i] = 1 mM. Since the ratio [ADP][P_i]/[ATP] is constant, $\Delta\mu$ is constant (see (1)) except for a minor difference of $\Delta\mu°$ due to changes in variables such as the ionic strength and concentration of free Mg^{2+}. The thick line corresponds to $\Delta\mu$ with indicating its estimation error as the line width. c, W_{stall} at [ATP] = 10 μM while varying [ADP] and [P_i] to control $\Delta\mu$. Error bars (standard errors) are smaller than the symbols. Adapted from ref. 9.

rotational rate decreased accordingly. Under a sufficiently strong torque, we observed rotation in the ATP-synthetic direction, with three steps per rotation. At an intermediate magnitude of torque, the probe particle showed bi-directional stepwise fluctuations with 120° steps and stalled on average. It is noteworthy that at this stalled state the rotation neither froze at a specific angular position nor displayed freely rotating Brownian motion. The stalled state is the state where rates of forward steps and backward steps are balanced.

Maximum work and thermodynamic efficiency

The stall torque, that is the torque necessary to stall the motor, multiplied by 120° is equivalent to the maximum work ($\equiv W_{stall}$) that the F_1-motor can perform per 120° rotation. On the other hand, the thermodynamic limit of the work extractable from an ATP hydrolysis is the free energy change liberated by a single ATP hydrolysis $\Delta\mu$:

$$\Delta\mu = \Delta\mu° + k_BT \ln \frac{[\mathrm{ATP}]}{[\mathrm{ADP}][\mathrm{P_i}]} . \qquad (1)$$

In other words, $\Delta\mu$ is the driving force of the F_1-motor's rotations. Figure 3b and c show that W_{stall} is nearly equal to $\Delta\mu$ under a variety of conditions except at extremely low [ATP] and [ADP]. This coincidence suggests that F_1-motor has nearly 100% thermodynamic efficiency for the conversion between the chemical free energy and mechanical work.

The 100% thermodynamic efficiency is not prohibited by thermodynamic laws. However, it is amazing that a machine that achieves it exists in cells and is working to synthesize ATP in our body.

Efficiency during rotations far from quasistatic process

The stalled state corresponds to a quasistatic process, where it takes an infinite time to proceed a step. Therefore, it is difficult to guess the practical meaning of this efficiency in cells. On the other hand, it is important to evaluate the free-energy conversion efficiency during rotations far from quasistatic process. Let W_{motor} be the work exerted by the motor to rotate the γ-shaft 120°. W_{motor} cannot exceed $\Delta\mu$ during ATP-hydrolytic rotation because of the second law of thermodynamics: $W_{\mathrm{motor}} \leq \Delta\mu$. Now, the question that arises naturally is how much W_{motor} does the motor extract from $\Delta\mu$ during ATP-hydrolytic rotations?

W_{motor} is not accessible directly. However, we can evaluate it by measuring the energy flow through the probe. In our experiment, we probed the γ-shaft's rotations with a large probe particle connected to the shaft with a soft elastic protein linker. In the ATP-hydrolytic rotations, W_{motor} is transferred to the probe via the linker's elastic energy and consumed through the probe's rotation. W_{motor} increases the probe's potential against load $\Delta U_{\mathrm{probe}}$ if the probe is subjected to external load and the rest dissipates as a heat from the probe to the environment Q_{probe}:

$$W_{\mathrm{motor}} = \Delta U_{\mathrm{probe}} + Q_{\mathrm{probe}}. \qquad (2)$$

The energy balance relation (2) suggests that we can evaluate W_{motor} by measuring $\Delta U_{\mathrm{probe}}$ and Q_{probe}. Note that this is possible only when the probe and γ-shaft are thermally insulated in the sense that the time scales of the motions of the probe and γ-shaft are well separated. If these time scales are similar and $\Delta\mu$ is small, W_{motor} calculated by (2) is no longer a work that is fully extractable and can exceed $\Delta\mu$[28,29]. The diameters of the probe and γ-shaft were about 300 nm and 2 nm, respectively in the present study. Since the rotational diffusion coefficient is proportional to the cubic of the object's diameter, our experimental system is supposed to satisfy this condition well.

$\Delta U_{\mathrm{probe}}$ is nothing but the torque on the probe times 120° with the sign depending on the rotational direction; positive in the ATP-hydrolytic rotations and negative in the ATP-synthetic rotations. On the other hand, heat measurement is usually difficult in such a microscopic system subjected to thermal fluctuations[12]. The motion of a colloidal particle in a viscous fluid is described by the overdamped Langevin equation: $0 = \Gamma v - \partial_x U(x,t) + \xi(t)$, where the right hand side correspond to the frictional force, potential force, and the thermal force, respectively from the left to right. The frictional coefficient Γ and the thermal force ξ(t) are connected by the relation $\langle\xi(t)\xi(0)\rangle = 2\Gamma k_{\mathrm{B}}T\delta(t)$, where δ(t) is the Dirac's delta function. Sekimoto defined the amount of heat dissipation per unit time in the Langevin systems as the microscopic energy exchange with the environment $J \equiv \langle[\Gamma v - \xi(t)]v\rangle$[12]. This reasonable definition satisfies the conventional thermodynamic laws[12]. However, it is difficult to measure J because it includes the stochastic thermal force $\xi(t)$ which is not accessible in experiments. Harada and Sasa derived an equality that enables us to evaluate J from quantities obtainable in experiments[30–33]. This equality connects the fluctuation and the response function of the probe's rotational rate to the heat dissipation. We applied a small periodic torque on the probe by the electrorotation method and measured the response function of the rotational rate (see Fig. 4a for the experimental procedure). The response function indicates how much the rotational rate changes when subjected to a small external torque. Comparing this response function with the fluctuation of the rotational rate, we evaluated the heat dissipation per 120° rotation Q_{probe} ($\equiv \frac{J}{3v_s}$), where v_s is the mean rotational rate and $3v_s$ is the mean stepping rate[6]. Figure 4b shows that W_{motor} is nearly equal to $\Delta\mu$ during ATP-hydrolytic rotations. This suggests that the F_1-motor achieves nearly 100% free-energy conversion efficiency even during rotations far from quasi-static process.

Mechanism of highly efficient free-energy conversion

Empirically, 100% efficiency is achieved only in the quasi-static process. At a finite-time operation, extra irreversible heat dissipates through microscopic degrees of freedom as a heat. However, molecular motor is itself microscopic and works at the energy scale of $k_{\mathrm{B}}T$. The motor possibly utilizes thermal fluctuations and controls microscopic energy flow to maximize its efficiency to near 100%.

In order to clarify the mechanism of such a high efficiency in a finite-time operation, we first look at the mechanochemical scheme of the F_1-motor's rotation. During the ATP-waiting state, each β subunit is at one of the following three different chemical states: with ATP, with ADP (and P_i), and empty[34,35] (Fig. 5a). The chemical states of the three β subunits rotate cooperatively due to the ATP binding, ATP hydrolysis, and the release of ADP and a phosphate. The β subunit has a hinge-like structure and bites a nucleotide at the hinge. Since the conformation of the β subunit varies with the bound nucleotide[14,36], the interaction potential between the $\alpha_3\beta_3$ ring and γ shaft rotates and drives the γ-shaft's 120° rotation. This picture leads to a simple model that the stepwise rotation is described as a Brownian motion on a potential corresponding to the ATP waiting state, wherein the potential's position shifts 120° upon the ATP binding (Fig. 5b).

We expect that the information about the mechanical potential profiles would provide a crucial clue to the mechanism behind the high efficiency. However, what we obtain

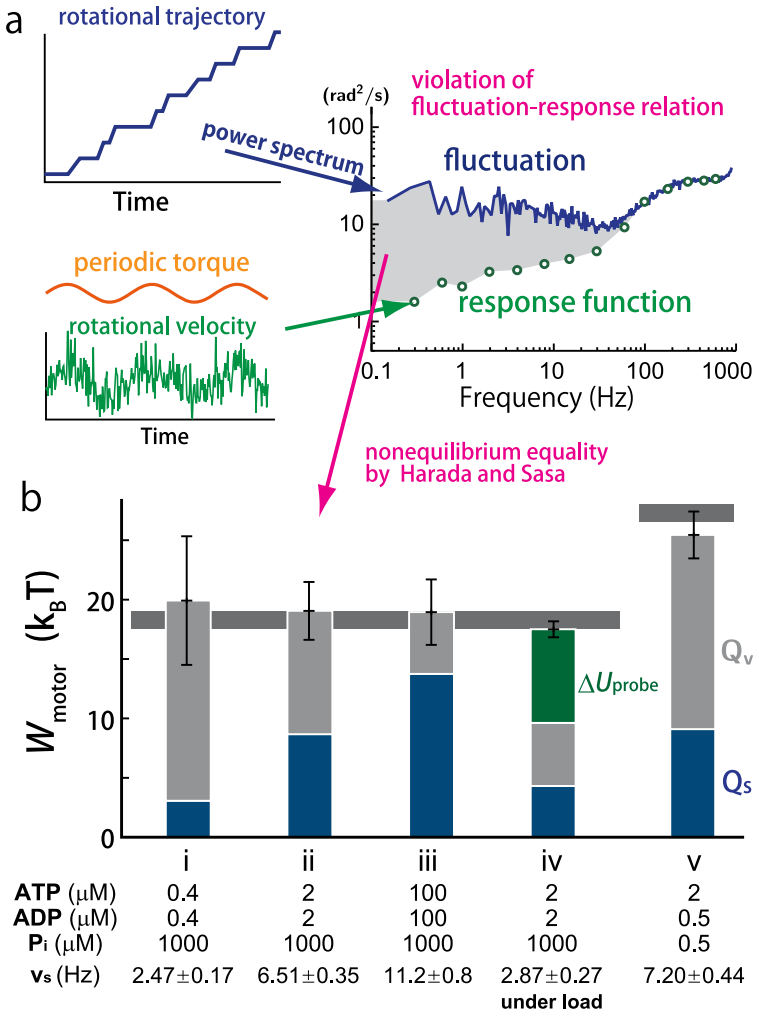

Figure 4 Measurement of W_{motor}. a, Measurement of Q_{probe} by Harada nad Sasa's equality. Fluctuation corresponds to the power spectrum of the rotational rate and is calculated from the rotational trajectory. The response function was mesaured by measuring the rotational rate under a small periodic torque at a broad range of frequencies. The Harada and Sasa's equality says that the difference between the fluctuation and response function multiplied by $2k_BT$ (corresponding to the shaded area) is proportional to Q_{probe}[6,30,31]. $Q_{probe} = Q_s + Q_v$ is plotted separately: the contribution from the steady motion Q_s and that from nonequilibrium fluctuations Q_v. Error bars indicate the standard deviations. Adapted from ref. 6 with modification.

in experiments is limited to the rotational trajectories of the probe. We developed a novel method to obtain the mechanical potential profile and the angular positions where the switchings of the potentials take place only from the trajectories on the basis of physically well-defined method[7]. Let $X \equiv (x_1, x_2, ..., x_L)$ be the observed trajectory, where L is the number of video frames. The core of this method is to estimate the chemical state sequence $S \equiv (s_1, s_2, ..., s_{L-1})$, where $s_i \in \{1, 2, 3\}$ is the chemical state assigned for the transition from the i-th to $(i+1)$-th video frame. We define a score function $\sigma(S, X)$ as the path probability of X and S (see ref. 7 for details). What we do is to estimate the chemical-state sequence S^* that maximizes $\sigma(S, X)$ for the given trajectory X. In experiments, $L \sim 1{,}000{,}000$. Therefore, it seems hopeless to find S^* from the 3^L possible chemical-state sequences. Whereas, the Viterbi algorithm based on the hidden Markov process modelling can find S^* at a computational cost of $O(3^2L)$, which depends on L linearly[37]. Hence, it dramatically reduces the computational cost. Once we know the chemical-state sequence, the mechanical potential is easily obtained from the trajectory by using the detailed-balance condition[7]. However, in the first place, the potential profile is necessary to compute the score function. We used an iteration method, where we assumed a harmonic potential as the initial guess of the potential profile and then estimated the chemical-state sequence. We iterated the potential-profile estimation and the chemical-state estimation until they converged.

Figure 6 shows the potential curves corresponding to each chemical state recovered only from the rotational trajectory. This method provides not only the mechanical potential curves but also the angular positions where the transitions occur. We found that transitions occur not randomly but in a limited region ahead of the potential minima

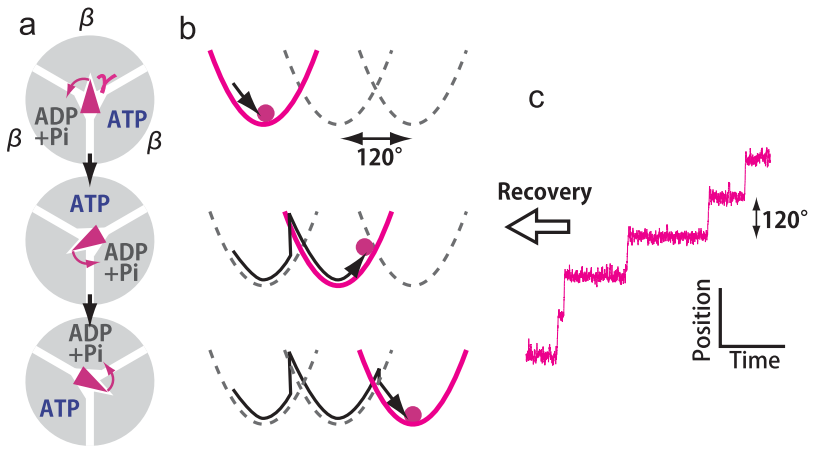

Figure 5 Recovery of potentials from single-molecule trajectories. a, Simplified reaction scheme of F_1-motor. α subunit is omitted for simplicity. The binding of ATP to the empty β subunit triggers 120° rotation. b, Interaction potentials between the γ shaft and β subunits. c, Single-molecule trajectory. We recover the potential profiles (b) only from single-molecule trajectories (c). Adapted from ref. 7.

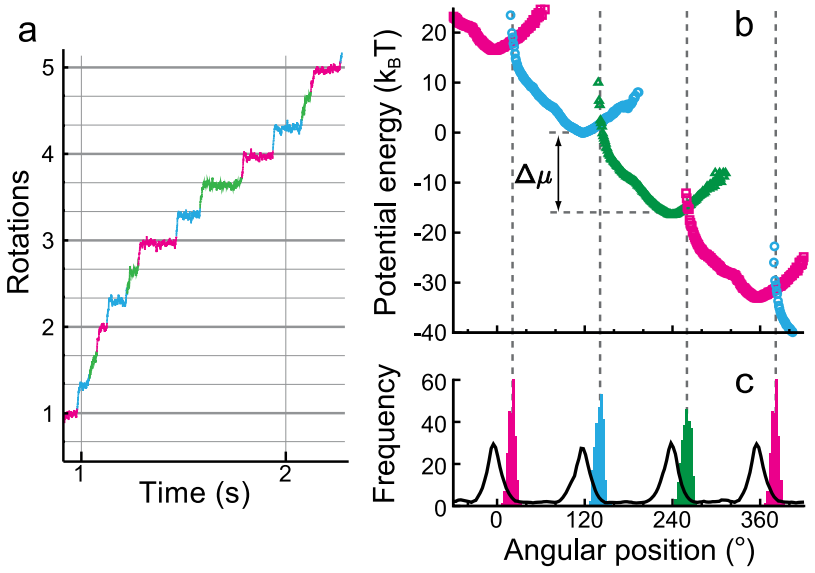

Figure 6 Recovered free-energy potentials and the angular distribution at transitions from the trajectory of an F_1-motor molecule. a, Rotational trajectory of the F_1-motor's probe particle observed at 9,000 Hz with an exposure time of 40 μs. The trajectory comprises approximately 650,000 frames. b, Recovered potentials corresponding to the ATP-waiting states. The vertical lines denote the intersection points of the potentials. The potentials are plotted with vertical shifts with the amount of the chemical free energy change of ATP hydrolysis ($\Delta\mu = 16.5\, k_BT$). c, Angular distribution at the transitions (histogram) and the overall angular distributions (solid line). The overall angular distribution is scaled by eye to be compared with the transition angular distributions. The potential profile in b and angular distribution at transitions from this state in c are depicted using the same colour. Adapted from ref. 7.

around the potentials' intersection points (Fig. 6c). That is, the F_1-motor changes its chemical state depending on the γ-shaft's angular position. Only when the transitions occur at around intersection points on average, $Q_{\text{probe}} \cong \Delta\mu$. This implies that the F_1-motor achieves the highly-efficient free-energy transduction by such an angular-position-dependent control of the chemical state.

Summary

We combined a response measurement of a single F_1-motor molecule and a recent nonequilibrium theory and evaluated the thermodynamic quantities of the F_1-motor at a single-molecule level. The 100% free-energy conversion efficiency is not prohibited by thermodynamic laws. However, it is usually reached only at the quasistatic limit such as a molecular motor at the stalled state[9] and a macroscopic cylinder with a piston pulled or pushed infinitely slowly. We

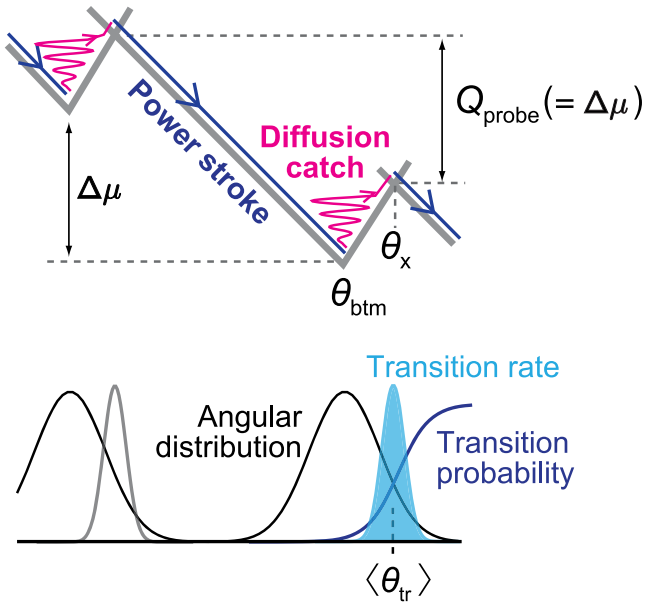

Figure 7 The torque generation by the F_1-motor. The F_1-motor shifts the potentials discontinuously depending on the γ-shaft's motion. The angular position of the γ-shaft fluctuates due to thermal motions. The heat through the rotations Q_{probe}, which was measured by using Harada-Sasa equality in Fig. 4, can be calculated as the potential change between successive transitions. When the transition is limited around θ_x, $\Delta\mu \cong Q_{probe}$. Adapted from ref. 7 with modification.

showed that F_1-motor achieves nearly 100% free-energy efficiency not only around the stalled state but even during rotations far from quasistatic process. When we pull or push a piston attached to a thermally-open macroscopic cylinder quickly, turbulence is inevitable and additional energy dissipates through microscopic degrees of freedom as an irreversible heat. This reduces the efficiency. On the other hand, F_1-motor is itself microscopic in the sense that it works in the energy scale of k_BT and can access microscopic degrees of freedom. Hence, the F_1-motor possibly utilizes thermal fluctuations and rectifies the energy flow in the k_BT scale. It was suggested that the F_1-motor shifts the mechanical potentials discontinuously depending on the γ-shaft's angular position instead of moving the potential infinitely slowly at a quasi-static limit (Fig. 7)[7]. Such an operation, which is possible only by nanosized machines, can minimize the irreversible heat and achieves a high efficiency even at a finite-time operation. This highlights the remarkable property of nanosized engines. However, it is still not clear how the motor realizes the angular-position-dependent control of the chemical state.

This work was supported by Japan Science and Technology Agency (JST) and Grant-in-Aid for Scientific Research on Priority Areas. S. T. was supported by Alexander von Humboldt foundation.

References

1. Bustamante, C., Liphardt, J. & Ritort, F. The nonequilibrium thermodynamics of small systems. *Physics Today* **58**, 43–48 (2005).
2. Jarzynski, C. Nonequilibrium equality for free energy differences. *Phys. Rev. Lett.* **78**, 2690–2693 (1997).
3. Evans, D. J., Cohen, E. & Morriss, G. Probability of second law violations in shearing steady states. *Phys. Rev. Lett.* **71**, 2401–2404 (1993).
4. Evans, D. J. & Searles, D. J. The fluctuation theorem. *Adv. Phys.* **51**, 1529–1585 (2002).
5. Jarzynski, C. Equalities and inequalities: irreversibility and the second law of thermodynamics at the nanoscale. *Annu. Rev. Condens. Matter Phys.* **2**, 329–351 (2011).
6. Toyabe, S., Okamoto, T., Watanabe-Nakayama, T., Taketani, H., Kudo, S. & Muneyuki, E. Nonequilibrium energetics of a single F_1-ATPase molecule. *Phys. Rev. Lett.* **104**, 198103 (2010).
7. Toyabe, S., Ueno, H. & Muneyuki, E. Recovery of state-specific potential of molecular motor from single-molecule trajectory. *EPL* **97**, 40004 (2012).
8. Muneyuki, E., Watanabe-Nakayama, T., Suzuki, T., Yoshida, M., Nishizaka, T. & Noji, H. Single molecule energetics of F_1-ATPase motor. *Biophys. J.* **92**, 1806–1812 (2007).
9. Toyabe, S., Watanabe-Nakayama, T., Okamoto, T., Kudo, S. & Muneyuki, E. Thermodynamic efficiency and mechano-chemical coupling of F_1-ATPase. *Proc. Nat. Acad. Sci. USA* **108**, 17951–17956 (2011).
10. Hayashi, K., Ueno, H., Iino, R. & Noji, H. Fluctuation theorem applied to F_1-ATPase. *Phys. Rev. Lett.* **104**, 218103 (2010).
11. Palanisami, A. & Okamoto, T. Torque-Induced slip of the rotary motor F_1-ATPase. *Nano Lett.* **10**, 4146–4149 (2010).
12. Sekimoto, K. *Stochastic energetics (Lecture Notes in Physics)*. (Springer, Berlin, 2010).
13. Seifert, U. Stochastic thermodynamics, fluctuation theorems, and molecular machines. *Rep. Prog. Phys.* **75**, 126001 (2012).
14. Abrahams, J. P., Leslie, A. G. W., Lutter, R. & Walker, J. E. Structure at 2.8 A resolution of F_1-ATPase from bovine heart mitochondria. *Nature* **370**, 621–628 (1994).
15. Boyer, P. D. The binding change mechanism for ATP synthase —some probabilities and possibilities. *Biochim. Biophys. Acta* **1140**, 215–250 (1993).
16. Yoshida, M., Muneyuki, E. & Hisabori, T. ATP synthase—a marvellous rotary engine of the cell. *Nat. Rev. Mol. Cell Biol.* **2**, 669–677 (2001).
17. Noji, H., Yasuda, R., Yoshida, M. & Kinosita, K. Direct observation of the rotation of F_1-ATPase. *Nature* **386**, 299–302 (1997).
18. Yasuda, R., Noji, H., Ishiwata, S., Yoshida, M. & Kinosita Jr., K. F_1-ATPase is a highly efficient molecular motor that rotates with discrete 120 Steps. *Cell* **93**, 1117–1124 (1998).
19. Rondelez, Y., Tresset, G. & Nakashima, T. Highly coupled ATP synthesis by F_1-ATPase single molecules. *Nature* **433**, 773–777 (2005).
20. Watanabe, R., Tabata, K. V., Iino, R., Ueno, H., Iwamoto, M., Oiki, S. & Noji, H. Biased Brownian stepping rotation of F_oF_1-ATP synthase driven by proton motive force. *Nat. Commun.* **4**, 1631 (2013).
21. Watanabe-Nakayama, T., Toyabe, S., Kudo, S., Sugiyama, S., Yoshida, M. & Muneyuki, E. Effect of external torque on the ATP-driven rotation of F_1-ATPase. *Biochem. Biophys. Res. Commun.* **366**, 951–957 (2008).
22. Hirono-Hara, Y., Ishizuka, K., Kinosita, K. Jr., Yoshida, M. & Noji, H. Activation of pausing F_1 motor by external forces. *Proc. Nat. Acad. Sci. USA* **102**, 4288–4293 (2005).

23. Itoh, H., Takahashi, A., Adachi, K., Noji, H., Yasuda, R., Yoshida, M. & Kinosita, K. Mechanically driven ATP synthesis by F_1-ATPase. *Nature* **427**, 465–468 (2004).
24. Gosse, C. & Croquette, V. Magnetic tweezers: micromanipulation and force measurement at the molecular level. *Biophys. J.* **82**, 3314–3329 (2002).
25. Washizu, M., Kurahashi, Y., Iochi, H., Kurosawa, O., Aizawa, S.-i., Kudo, S., Magariyama, Y. & Hotani, H. Dielectrophoretic measurement of bacterial motor characteristics. *IEEE Trans. Ind. Appl.* **29**, 286–294 (1991).
26. Toyabe, S., Sagawa, T., Ueda, M., Muneyuki, E. & Sano, M. Experimental demonstration of information-to-energy conversion and validation of the generalized Jarzynski equality. *Nature Phys.* **6**, 988–992 (2010).
27. Berry, R. M., Turner, L. & Berg, H. C. Mechanical limits of bacterial flagellar motors probed by electrorotation. *Biophys. J.* **69**, 280–286 (1995).
28. Zimmermann, E. & Seifert, U. Efficiencies of a molecular motor: a generic hybrid model applied to the F_1-ATPase. *New Journal of Physics* **14**, 103023 (2012).
29. Wang, H. & Oster, G. The Stokes efficiency for molecular motors and its applications. *Europhys. Lett.* **57**, 134–140 (2002).
30. Harada, T. & Sasa, S. Equality connecting energy dissipation with a violation of the fluctuation-response relation. *Phys. Rev. Lett.* **95**, 130602 (2005).
31. Harada, T. & Sasa, S. Energy dissipation and violation of the fluctuation-response relation in non-equilibrium Langevin systems. *Phys. Rev. E.* **73**, 26131 (2006).
32. Toyabe, S., Jiang, H. R., Nakamura, T., Murayama, Y. & Sano, M. Experimental test of a new equality: measuring heat dissipation in an optically driven colloidal system. *Phys. Rev. E* **75**, 2–5 (2007).
33. Toyabe, S. & Sano, M. Evaluating energy dissipation of a brownian particle in a viscoelastic fluid. *Phys. Rev. E* **77**, 41403 (2008).
34. Adachi, K., Oiwa, K., Nishizaka, T., Furuike, S., Noji, H., Itoh, H., Yoshida, M. & Kinosita, K. Jr. Coupling of rotation and catalysis in F_1-ATPase revealed by single-molecule imaging and manipulation. *Cell* **130**, 309–321 (2007).
35. Watanabe, R., Iino, R. & Noji, H. Phosphate release in F_1-ATPase catalytic cycle follows ADP release. *Nat. Chem. Biol.* **6**, 814–820 (2010).
36. Masaike, T., Koyama-Horibe, F., Oiwa, K., Yoshida, M. & Nishizaka, T. Cooperative three-step motions in catalytic subunits of F_1-ATPase correlate with 80 and 40 substep rotations. *Nat. Struct. Mol. Biol.* **15**, 1326–1333 (2008).
37. Press, W. H., Teukolsky, S. A., Vetterling, W. T. & Flannery, B. P. *Numerical Recipes Third Edition* (Cambridge University Press, Cambridge, 2007).